



HAL
open science

A Chronology of Marl Pits in the Paris Basin Determined from the Infilling of Closed Depressions: Do Marling Practices Have Their Origin in the Neolithic Period?

Brasseur Boris, Théo Allalou, Laurent Chalumeau, Emilie Gallet-Moron,
Jérôme Buridant

► To cite this version:

Brasseur Boris, Théo Allalou, Laurent Chalumeau, Emilie Gallet-Moron, Jérôme Buridant. A Chronology of Marl Pits in the Paris Basin Determined from the Infilling of Closed Depressions: Do Marling Practices Have Their Origin in the Neolithic Period?. 2022. hal-04469216

HAL Id: hal-04469216

<https://hal.science/hal-04469216>

Preprint submitted on 20 Feb 2024

HAL is a multi-disciplinary open access archive for the deposit and dissemination of scientific research documents, whether they are published or not. The documents may come from teaching and research institutions in France or abroad, or from public or private research centers.

L'archive ouverte pluridisciplinaire **HAL**, est destinée au dépôt et à la diffusion de documents scientifiques de niveau recherche, publiés ou non, émanant des établissements d'enseignement et de recherche français ou étrangers, des laboratoires publics ou privés.

1 **A chronology of marl pits in the Paris Basin determined from the infilling of**
2 **closed depressions: do marling practices have their origin in the Neolithic**
3 **period?**

4 Boris Brasseur¹, Théo Allalou¹, Laurent Chalumeau¹, Emilie Gallet-Moron¹, Jérôme Buridant¹.

5 ¹ Ecologie et Dynamique des Systèmes Anthropisés (EDYSAN, UMR CNRS 7058), Université de

6 Picardie Jules Verne, Amiens, France

7 Corresponding author: boris.brasseur@u-picardie.fr

8 **Abstract**

9 Marling (limestone alkaline amendment) agrarian practices have a plurimillennial influence on
10 soil pH and on soil-associated ecosystems. Although the earliest written records in Europe
11 date back to antiquity, the origin of this agrarian practice is not well known. In order to trace
12 the evolution of this practice in the early agrarian societies of Western Europe, we searched
13 for topographic anomalies of ancient limestone quarries that may have been used for marling.
14 Several hundred circular closed topographic depressions (CCDs) were identified under two
15 areas of ancient forest in northern France with Lidar digital elevation models (DEMs). Soils,
16 morphology and archaeological context were studied and filling sediments were dated in
17 several dozen CCDs.

18 The gaps in the carbonate rocks, soils with calcaric properties (scattered limestone fragments),
19 unstratified fills, the absence of buried paleosols, and dates (OSL, C-14) later than the first
20 local agricultural societies made it possible to recognise the CCDs that may have served as
21 limestone quarries. This was the case for most of the 30 CCDs studied, leaving a minority of
22 natural origin (suffosion, depressions of thermokarstic origins). Amongst the quarries

1 identified, the preferential excavation of soft (friable) limestone and the localization of these
2 quarries in fossil agrarian plots led us to hypothesize that they were used for alkaline
3 amendments of the cultivated fields. The quarries were filled from the Middle Neolithic to
4 Late Antiquity, shortly before the period of afforestation of these former agrarian territories.

5

6 **Keywords**

7 Lidar, topographic depression, limestone quarry, calcaric, technosol, soil alkalisation.

8

9

10

11

12 **1. Introduction**

13 Many plant species in food crops require near-neutral soil pH conditions for optimal growth and yields.
14 Marling or liming of soils is practised in agriculture to neutralise soil acidity and improve nutrient
15 availability (Läuchli and Grattan, 2017; Matthew, 1993). This practice is particularly relevant in areas
16 where soils are subject to natural acidification when rainfall exceeds evapotranspiration (Slessarev et
17 al., 2016). The most common materials used for marling are various limestones in granular (friable or
18 fragmented) form and their derivatives such as lime (Goulding, 2016). However, in the absence of
19 these materials, farmers may also use sandy deposits of calcareous seaweed (Clout and Phillips, 1972)
20 or the alkaline plant ash (Juo and Manu, 1996) during slash and burn practices.

21 For all soils undergoing acidolysis and acido-complexolysis processes, the practice of marling will
22 constitute a revolution in the dynamics of functioning processes. Due to the increase of pH and the

1 availability of Ca, processes such as argilluviation will stop, cation exchange capacity will raise,
2 structural stability will increase, and so will the anecic earthworm populations (Chauchan, 2014; IUSS
3 Working Group WRB, 2015; Quénard et al., 2011). Soil marling is therefore a practice that structures
4 pedogenetic dynamics over time.

5 In north-western Europe, marling with limestone is an ancient agronomic practice first described by
6 Varron in the first century BC (Cato the Elder, Varon, Columella, & Palladius Ed. 1864: Book I—Chapter
7 VIII). Later, in a much more detailed treatise, Pliny the Elder (Pliny the Elder, 1877: Book XVII—Chapter
8 4) described the use of various calcareous rocks (called *margam*) for marling in Germany, France and
9 Britain. For example he mentions the use of various limestones such as *columbina* (pigeon grey), *rufa*
10 (reddish), *argillacea* (heavy marl), *tofacea* (tufa), *harenacea* (sandy), *calce* (lime). These are used
11 primarily for cereals (tufa, chalk and white limestone) but also for fodder (heavy marl) (Winiwarter and
12 Blum, 2008).

13 Thus, since antiquity, marling has been carried out with a variety of carbonate rocks suitable for
14 alkaline amendments in fields, and not only with marl. The choice of the calcareous rock, rather sandy
15 or clayey, could then be justified by an improvement of the soil texture for the envisaged agronomic
16 use (Pliny the Elder, 1877: Book XVII—Chapter 4; Young, 1808). These practices still have a measurable
17 impact on soil pH and Ca content several thousand years after their abandonment (Brasseur et al.,
18 2018, 2015).

19 The antiquity of the marling practice is largely unknown but potential relics of the activity exist in the
20 form of old limestone quarries used for these amendments (Prince, 1961). After their abandonment,
21 the quarries were being partially buried and now appear as closed depressions (CDs), more or less
22 levelled in the landscape. Gillijns et al (2005) described depression forms under forest cover and in
23 open fields in Belgium and noted their erasure on the fields/crops. They also indicate an anthropogenic
24 origin for eight out of 26 CDs, used as limestone, iron or sand quarries, and for some, as limestone

1 loess quarries. The authors seriously considered the hypothesis that the quarries used to serve for
2 calcareous/alkaline amendments for crop improvement.

3 In the Merdaal forest (central Belgium), Vanwalleghem et al. (2007) dated the colluvium infill of a CD
4 between the first century BC and the fourth century AD. The CD was contemporary with local
5 agricultural activities, inferred from gully infills dated from the 18th century BC to the third century
6 AD. The authors attributed the excavation of the calcareous loess in the local CDs to the practice of
7 marling. Near the same forest, Rommens et al. (2007) dated the colluvium infill of one of these
8 anthropogenic CDs to the Middle Bronze Age (1120-900 BC). Meylemans et al. (2014) also reported
9 similar CDs, without dating the infill, in the vicinity of the Middle Neolithic site of Ottenburg (Central
10 Belgium).

11 In western Germany (Baumewerd-Schmidt and Gerlach, 2001) and in Britain (Prince, 1961), other CDs
12 have been recognised as marl pits, but no further information on their age is available.

13 Other CDs of anthropogenic origin had multiple functions compatible with a possible initial use as
14 marling. Thus, in the North-East of France (Etienne et al., 2011), CDs on marl were probably later used
15 for watering herds and/or for retting flax. The filling of the CDs studied dates from the Iron Age to the
16 Roman period. Some of these CDs could also be of natural origin following the dissolution of diapirs or
17 the subsidence of the soil. These findings were complemented by other work in Luxembourg
18 (Slotboom and van Mourik, 2015; van Mourik et al., 2016), where an anthropogenic origin was found
19 in some cases, with possible clay quarries for ceramics. The age of the fills in these quarries ranges
20 from Roman times to the Middle Ages. The absence of buried paleosols under/inside the colluvium
21 infill is the sign of a CD of anthropogenic origin.

22 Kołodyńska-Gawrysiak & Poesen (2017) carried out an overview of the work on CDs in the loess belt in
23 Europe. The analysis of Eastern European CDs mainly suggests natural landforms (from loess deflation,
24 dissolution, thermokarst processes). According to ¹⁴C datings, the CDs in eastern Poland were formed
25 between the Late Glacial and the mid-Holocene period. The morphometric characteristics, ages and

1 stratigraphy of the infills clearly indicate that natural thermokarstic depressions were filled by colluvial
2 deposits due to agricultural land use in the second half of the Holocene. The presence of mid-Holocene
3 mature paleosols (Chernozems, Phaeozems, Luvisols or Albeluvisols) buried under the colluvium
4 infilling also points to an ancient natural origin of the CDs (Kołodzyńska-Gawrysiak, 2019). In Western
5 Europe, a dominant anthropogenic origin (i.e. loess and limestone quarries, underground quarry
6 collapses, bomb and mine craters) is more common for CDs. But natural landforms such as sinkholes,
7 salt lenses and limestone dissolution dolines have also been reported (Delafosse, 1948), especially in
8 the Paris region (Pissart, 1958).

9 To sum up, the similar surface forms resulting from this wide variety of CDs constitutes a possible
10 confusing factor in the interpretation of these structures. Systematic investigation of the fillings and
11 their dating is therefore necessary.

12

13 Cereals, originating from the Near East, are cultivars adapted to local neutral-alkaline soils and must
14 therefore have required soils with neutralised acidity from the beginning. Our hypothesis is that the
15 practice of marling is much older than the antiquity period because the first farmers in Northwest
16 Europe had to adapt the chemical qualities of naturally acidic soils to the plants they cultivated. We
17 believe that in former agrarian territories the anthropic impact of marling on the soils is often
18 underestimated and that this practice has strongly and durably structured the characteristics of
19 soils where it has developed.

20 Our objective was to date a set of filled marl pits in the north-central part of the Paris basin in order to
21 estimate the age of the soil marling practices. To identify a maximum number of marl pits, we targeted
22 i) former agrarian territories where CDs are abundant, ii) depressions under forest cover where the
23 ancient agrarian microtopography is better preserved (Lenoir et al., 2022), and iii) areas where the
24 subsoil would have been favourable for marling.

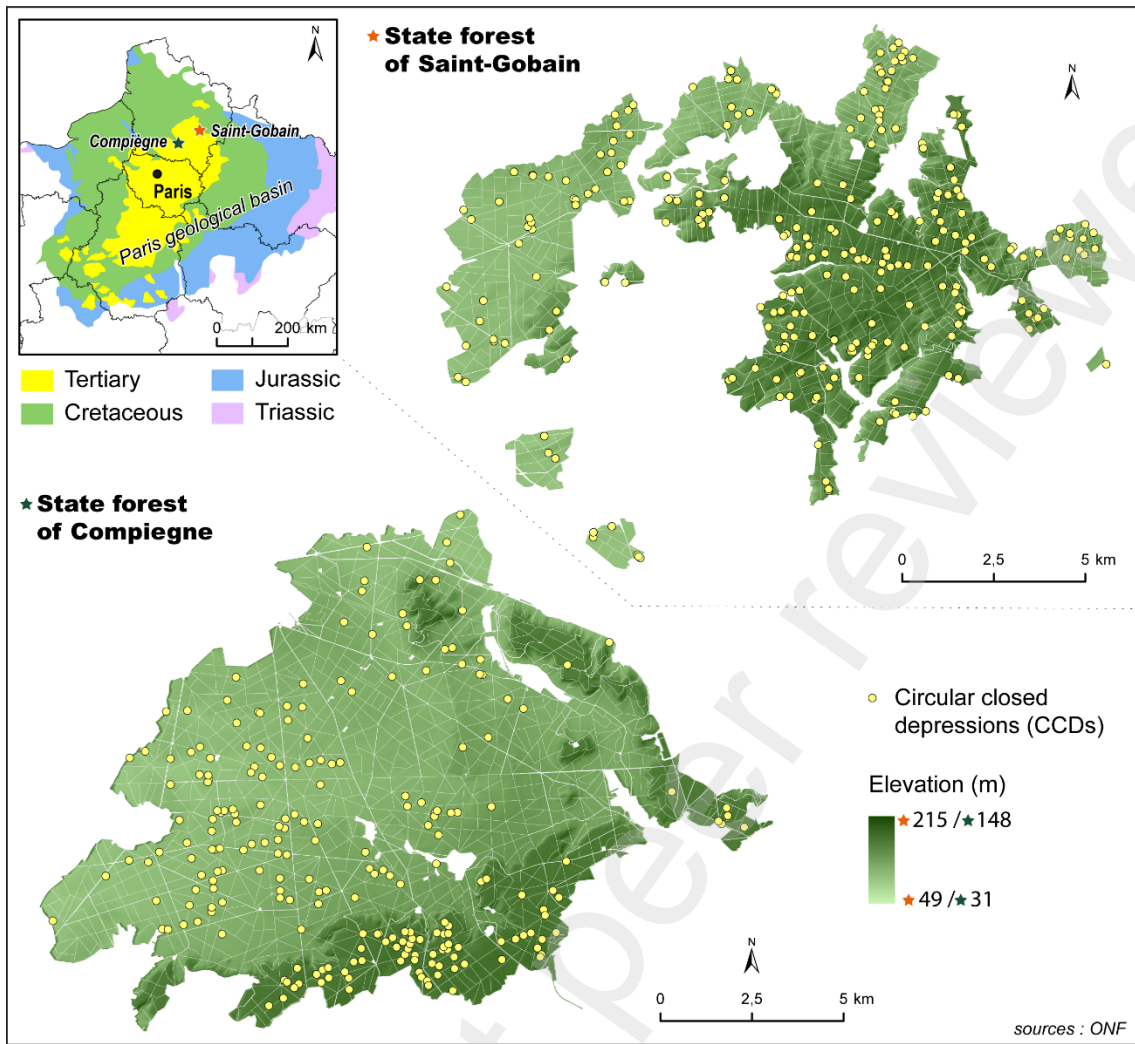
1 In order to identify the origin of the CDs, we studied their infilling (stratigraphy), their pedological
2 contexts and the contact with the local limestone substratum. To date the selected CDs, we decided
3 to analyse the lowermost infillings with Optically Stimulated Luminescence (OSL) and carbon 14 (¹⁴C)
4 when rare charcoal remains were discovered.

5 We selected two large woodland areas, Compiègne and Saint-Gobain forest massifs, exhibiting a high
6 diversity of soil types over contrasted geological substrates, making available the targeted limestone
7 properties. The geological strata in these forests are relatively thin and have a lateral variability in the
8 facies that makes it easier to discern the strategies used by former inhabitants for the acquisition of
9 carbonate rocks and the characteristics they sought. Both forests were agricultural areas during the
10 Roman period and probably even a few centuries before. High-resolution lidar DEMs enabled us to
11 locate and then determine the geomorphological and fossil agrarian context of the observed CDs.
12 Finally, it should be noted that karstic networks are very rare in the limestone areas in the northern
13 Paris Basin (Rodet, 2010), which limits the risk of natural sinkholes forming on the surface.

15 **2. Material and methods**

16 **2.1. Study sites, past and present contexts**

17 The forests of Compiègne and Saint-Gobain are located in the north-central part of the Paris basin (Fig.
18 1). The first farming populations settled around 4500 BC in the Oise valley bordering the current
19 territory of the two forests (Leroyer, 2006; Leroyer et al., 2017). Field surveys, complemented by a
20 remote sensing survey with Lidar technology (David and Dardignac, 2018), carried out on the two
21 forests revealed hundreds of Roman sites, mainly rural settlements, within the forests (Pichon, 2002;
22 Thuillier, 2017).



1

2 Fig. 1. Sitemap of the Saint-Gobain and Compiègne forests in the north-central part of the Paris
 3 geological basin. The yellow dots correspond to the circular closed depressions (CCDs) identified thanks
 4 to the DEMs of Lidar surveys.

5

6 The Gallo-Roman settlements were abandoned rather abruptly towards the end of the 4th century AD,
 7 with archaeological evidence of destruction and fires as early as the 3rd century AD (Fremont and
 8 Woimant, 1976, 1975; Tuffreau-Libre, 1977). On the territory of the Compiègne forest, a woodland is
 9 mentioned for the first time in the 6th century by Grégoire de Tours (de Tours, 1836); the forest then
 10 became a royal hunting reserve until the French revolution in 1789 AD. The Saint-Gobain forest was
 11 part of the Voas forest in the early Middle Ages (*Acta Sanctorum, Vita Sancti Gobani*). The study of the

1 local Lidar DEM reveals numerous Gallo-roman agricultural parcels. This forest therefore probably
2 developed between the final period of the Western Roman Empire and the early Middle Ages.
3 Today, the local climate is sub-oceanic with an average annual temperature of 10.5°C and an annual
4 rainfall of 650 mm (Climate-data.org, n.d.). Acidolysis and acidocomplexolysis are the two main
5 geochemical soil-forming processes. The geological substratum is mainly composed of marine tertiary
6 tabular sedimentary rocks (Thanetian to Barthonian), sometimes covered by more recent continental
7 deposits (Pleistocene to Holocene). In both forests, the three dominant soil groups are Cambisol,
8 Luvisol and Podzol. In the 20th century, a 1200-ha plateau area south of the Compiègne forest, mostly
9 covered with fields, was supplied with limestone by three marl pits (Guérin et al., 1975). These pits
10 exploited Middle-Upper Lutetian limestone and were all closed towards the end of the 20th century.
11 This recent situation indicates a rarefication of marl pits over two centuries (Clout and Phillips, 1972;
12 Matthew, 1993).

13 **2.2. Field survey, laboratory analyses and data analyses**

14 Around 150 and 250 circular closed depressions (CCDs) have been characterized within Compiègne
15 (14,357 ha) and Saint-Gobain (8,470 ha) forests, respectively, thanks to airborne Lidar DEMs (hillshade
16 models with two mutually perpendicular directions). The realisation of the shaded DEM and the
17 calculation of depth, area and diameter of CCDs were carried out with the ArcGis Pro 2.8 software
18 (ESRI).

19 In the Compiègne forest (FDC), among the 150 CCDs recorded on the DEM, a high density is observed
20 on the southern plateau (Fig.1). Finally, only the central and eastern parts of the forest, with upper
21 Pleistocene blown sand formations, have few CCDs. It is also on these siliceous sand dunes that the
22 absence of agrarian parcelling and other archaeological structures had previously been noted (Horen
23 et al., 2015). In the Saint-Gobain massif (SGB), where such thick dune formations are absent, the 250
24 CCDs are more equally distributed.

1 We selected CCDs that were sub-circular, over 10m in diameter, outside the areas of ancient
2 settlements and did not include bomb holes (characterised by smaller, rounder and sharper holes). We
3 then studied the infillings of 30 of these CCDs in various geological contexts, ranging from plains
4 (minimum altitude 48m) to plateaus (maximum altitude 170m).

5 For each CCD, hand auger cores were taken both inside and outside the depression i) until the first
6 hard rock is encountered irrespective of the depth; ii) to 1.5-metre-deep inside *in situ* carbonate soft
7 rocks; or iii) to 6m deep in other cases. Outside the CCDs, we determined the "local reference" for soil
8 and substrate rocks through (at least) one auger survey. Within the CCDs, two boreholes (auger and/or
9 soil pit) were drilled or dug to characterise the infills. We removed the CCDs with no carbonate rocks
10 outside and inside the depression in the first five metres and those where local carbonated rocks
11 appeared to be intact in the CCD footprint. We assumed the remaining 25 CCDs were potential marl
12 pits and therefore retained them for further investigation.

13

14 Based on this survey and with the help of the DEM, several morphological characteristics were
15 collected for the 25 CCDs: average elevation at the centre and outside of the CCDs; average diameter
16 and circularity ($\text{Perimeter}^2 / (4 * \pi * \text{Area})$); thickness of the infill in the CCDs; thickness of the
17 limestone gap; minimum depth of the carbonate fragments in the fill; and relative infill ratio (Infill
18 thickness/(Delta topographic + Infill thickness)). The infill thickness of the CCDs was defined as the
19 depth required to reach the unworked carbonate rock at the centre of the depression. Outside the
20 CCDs, we also measured the depth of the local soil and the thickness of any underlying soft limestone.

21 Seventeen were chosen for dating purposes; a trench was dug inside these CCDs to 1.5/2.2m in depth
22 or to the first hard rock substrate. A description of the pedogenetic, sedimentary and stratigraphic
23 characteristics of the CCD infilling was then carried out on the soil profiles obtained. Soil horizons and
24 sediment units were characterised in the field (based on colour, texture, structure, spatial
25 relationships) and following the World Reference Base for Soil Resources (IUSS Working Group WRB,

1 2015). In order to obtain a complete nomenclature of the horizons adapted to the description of the
2 diversity of the underlying source rocks, we also described the sequences of horizons according to the
3 French pedological reference system (AFES 2009). We also carried out pH analyses on the soils (5, 25
4 and 50cm depth) inside and outside the CCDs and measured CaCO_3 levels with a Bernard calcimeter
5 (volumetric method) on the same soil samples and on the calcareous substrates in the CCDs. Soil pH
6 was measured with two glass electrodes in distilled water (ISO 10390:2004) on two subsamples, then
7 averaged. We performed a Wilcoxon pairwise comparison rank test to evaluate differences in pH_{water}
8 values in the soils inside and outside the CCDs soils. All statistical analyses were performed within the
9 R software environment (R Development Core Team, 2016), with the “ggplot2”, “psych” and “corrplot”
10 packages.

11 Of the 17 CCDs, 16 were dated by OSL (n=14) or/and ^{14}C (n=4). OSL dates were established by the
12 Luminescence Dating Laboratory of the Silesian University of Technology, Gliwice. Multigrain
13 measurement of quartz grains (125-200 μm) was realised following the single aliquot regenerative
14 method for 16 aliquots and a “Central Age Model” was established (Galbraith et al., 1999). ^{14}C dating
15 was carried out following the AMS method at the Poznań Radiocarbon Laboratory. The calibration was
16 done on the OxCal software v4.4.2 (Ramsey, 2009) and with atmospheric data from Reimer et al
17 (Reimer et al., 2020).

18

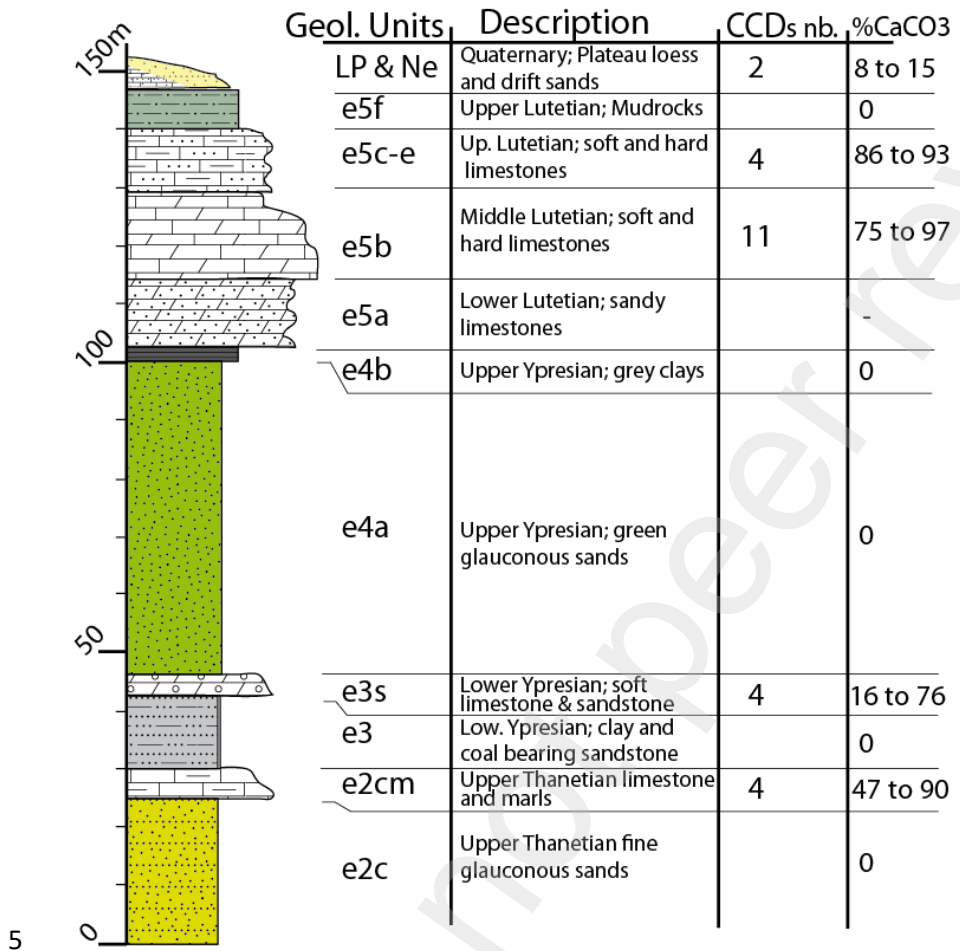
19 **3. Results**

20

21 **3.1. Geological context & carbonate rocks gaps**

22 Within the 25 CCDs, gaps (compared to their surroundings) were observed for several carbonate rock
23 facies: loess (2), Lutetian limestone (15), Ypresian coarse limestone and “faluns” (4), and Thanetian
24 limestone and marl (4) (Fig. 2). Loess has a relatively low carbonate content (8-15%) whereas Lutetian

1 limestones can reach 97% CaCO₃. Of the 25 CCDs, 18 were dug at the expense of soft (granular to
 2 friable) limestone material. In the case of the CCDs present on the Lutetian limestone, 9 CCDs (FDC-
 3 CCD1, 2, 3, 4, 5, 9, 10, 12; SGB-CCD4, CCD8) have a flat bottom (sometimes with a slight slope from the
 4 centre to the edges) composed of massive hard limestone bedrock.



6 Fig. 2: Stratigraphic log of the global sequence of Tertiary rock found in the Compiègne and Saint-
 7 Gobain forests. White rocks with brick-like features correspond to calcareous rocks. The 25 CCDs with
 8 limestone gap were counted for these different limestone facies on the log. Thickness data and
 9 descriptions are taken from the 1:50,000 geological maps of "Attichy" and "La Fère" (BRGM). The % of
 10 CaCO₃ corresponds to the calcium carbonate content we measured with the Bernard calcimeter or
 11 was taken from published data in the local geological map records.

12 **3.2. Closed depressions: morphology and relative infilling**

1 On the Lidar DEM, the 25 candidate CCDs for marls pits have sub-circular shapes. Their circularity index
2 ranges from 1.02 to 1.19. Regarding their average diameters, they vary from 55.5m to 28.5m and their
3 topographic depths (relative to the average local ground elevation) from -320cm to -60cm. No positive
4 relief of extracted soil is associated with these CCDs, so if it was extracted, the exceeding earth appears
5 to have been spread further beyond. The thicknesses of the calcareous rocks gaps range from 65 to
6 335cm. Finally, the thickness of the sedimentary fill in the CCDs varies from 360 to 25cm and their
7 relative infill ratio from 0.09 to 0.82.

8 Analysis of the morphological features of the CCDs reveals that the sharpest and deepest topographic
9 depressions are those with the lowest infilling ratio (e.g. FDC-CCD1 to CCD4, Fig. 3). Conversely, the
10 shallow marked depressions have a higher infilling ratio. Thus, two opposing morphotypes are
11 distinguished, one with a well-defined recessed relief and a relatively thin infilling, while the other has
12 a faint relief but a much thicker filling. FDC-CCD1 and CCD3 illustrate these two opposite morphotypes
13 (supplementary data, Fig. A.1).

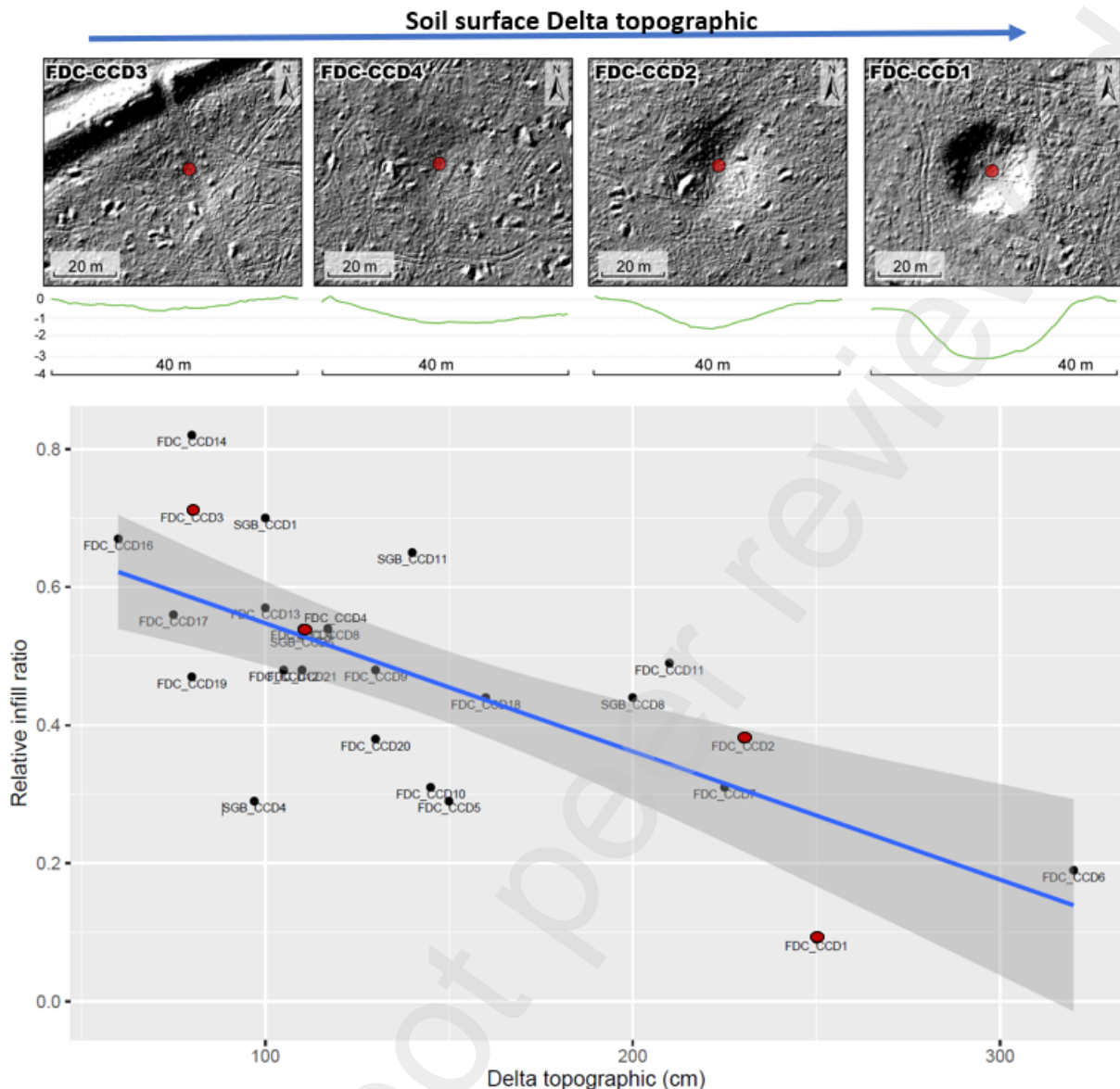
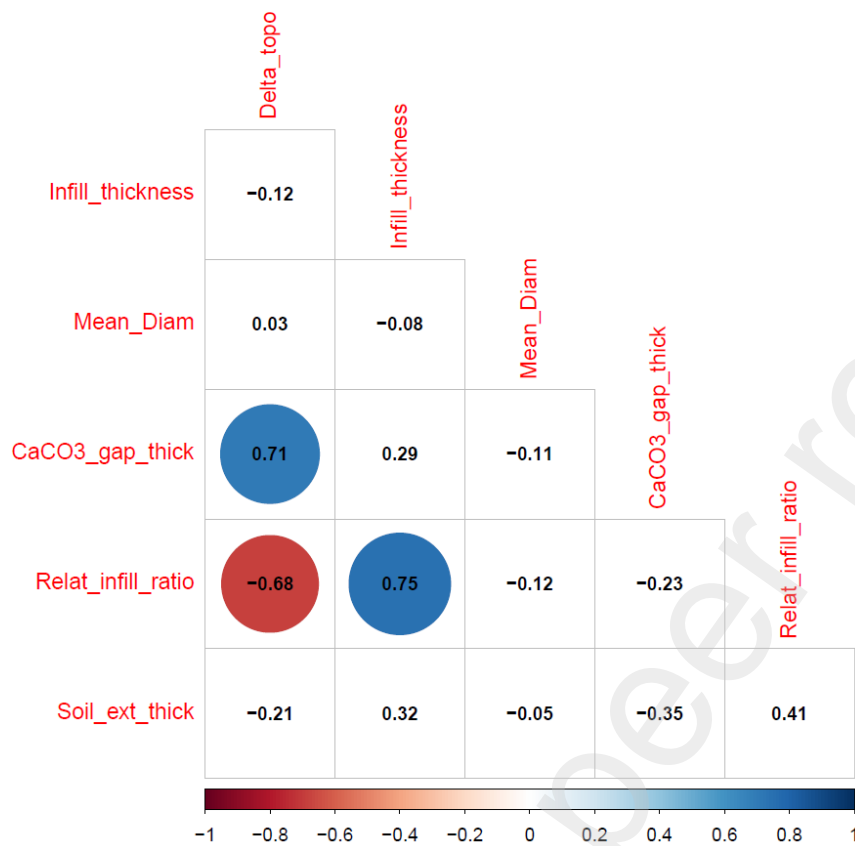


Fig. 3. Top: The topographic profiles of the four CCDs with red points illustrate the diversity of landforms encountered. Bottom: Graph representing the distribution of CCDs as a function of two variables, on the X-axis the difference in altitude (in centimetres) on the Lidar DEM between the centre of the CCD and the outside, and on the Y-axis the Relative infill ratio. The projected regression line with confidence intervals (shaded area) shows a negative relationship between these two variables.

The correlation matrix below (Fig. 4) also shows a positive correlation between the CaCO_3 thickness deficit and the topographic depth of the CCDs and a negative correlation between the topographic depth and the relative infill ratio. We can also observe that the CCDs will be more filled

- 1 (Relat_infill_ratio & Infill_tchick) if the external soils are thick. Finally, these soils will become thinner
- 2 if a significant thickness of carbonate rock has been extracted (CaCO3_gap_thick).



3

4 Fig. 4. Six morphological features of the 25 CCDs are compared in this correlation matrix with Spearman

5 correlation coefficients. These include the difference in elevation between the outside and centre of

6 the CCD on the Lidar DEM (Delta_topo), the thickness of the infill (Infill_thickness), the average

7 diameter (Mean_Diam), the thickness of the carbonate rock gap (CaCO3_gap_thick), the relative infill

8 ratio (Relat_infill_ratio), and the thickness of the soils surrounding the CCD (Soil_ext_thick). See in

9 supplementary data, Fig. A.2 for the histogram of the distribution of values per variable and the graphic

10 projections for the different pairs of variables.

11 Among the 25 marl pits, one of them (FDC-CCD1) had almost no fill, which allowed us to use it as an

12 example to describe the morphology of the contact between bedrock and fill for the entire CCD. FDC-

13 CCD1 is a relatively deep CCD (250cm) with a particularly shallow fill (20-30cm) and steep sloping

14 edges. The low fill revealed the general shape of the contact with the un-removed soil and rock. In this

1 CCD, we therefore noticed a lower slope on one sector of the southern edge. A 80 cm-deep soil pit was
2 made at this point. This revealed a steep boundary with a dense level of limestone fragments
3 associated with few pieces of reworked soils and some charcoal under the fill composed of soil and
4 few limestone fragments. The high degree of compaction of this level strongly resembles a trampled
5 surface. This surface follows a gentle slope from the outside to the inside of the depression.

6 **3.3. Infilling sequences: description and dating**

7 We described 17 CCDs infillings by assessing excavated trench walls and a complementary augering
8 survey (supplementary data, Fig. A.3). Particular attention was paid to breakage phenomena in the
9 filling sequences of the CCDs, whether they were stratifications, the formation of a soil, or cross-cutting
10 by secondary excavations. Among the 17 CCDs, only one (FDC-CCD11) had a buried soil horizon,
11 indicating a stable pedogenesis step inside the total infilling sequence. At the base of the infilling, we
12 found a 40cm-thick buried leptic calcaric pretic Anthrosol. We retrieved some roman archaeological
13 material into this thin buried soil layer (ceramic plate and earthenware fragments, charcoal, flint chips).
14 In the case of the CCDs SGB-CCD1 and SGB-CCD11, a sub-horizontal discontinuity intersected the
15 deposits of a previously formed fill. This could indicate a local secondary excavation, possibly related
16 to the installation of a charcoal kiln platform during recent forestry history. With the exception of FDC-
17 CCD11, the absence of an intercalated pedogenetic layer in 15 out of 16 infill sequences indicates
18 single-phase events.

19 The charcoal and datable archaeological artefacts (ceramics) found in the pits all predate the infilling
20 event. However, when these elements are present close to the soil surface (<100cm), this may indicate
21 more recent contamination by bioturbation (biogalleries, windfalls). This was the case for four CCDs
22 (FDC-CCD6 and CCD8, SGB-CCD1 and CCD8) where kilns had been installed on the soil surface. Some
23 pieces of charcoal had reached depths of nearly one metre from much more abundant accumulations
24 near the surface (<25cm). In such situations we did not consider these coals for the dating of the CCDs
25 fill.

1 Optically stimulated luminescence thermochronometry (OSL) tube sampling was carried out towards
 2 the base of the depression fill. Multi-grain quartz dating of the samples yielded ages between 28.9 and
 3 1.793 kyrs BP (Table 1). Six dates were between 28.900 and 12.710 kyrs BP; that is towards the end of
 4 the Late Pleistocene. The remaining eight dates were in the second half of the Holocene, from 5.850
 5 to 1.793 kyrs BP.

6 **Table 1** Dating results of CCD basal infillings. OSL ages stated are expressed in years before 1950.

Forest	CCD n°	Depth (m)	Material	Th-232 (Bq/kg)	228U (Bq/kg)	40K (Bq/kg)	Total Dose rate (Gy/kyrs)	Equivalent dose DE (Gy)	Age OSL (Kyr Before 1950)
FDC	CCD3	1.5	Quartz very fine sand	27	30.1	301	2.016	4.99	2.400(+/-0.013)
FDC	CCD4	1.1	Quartz very fine sand	31.5	45.2	288	2.24	4.18	1.793(+/-0.086)
FDC	CCD9	1.2	Quartz very fine sand	18.3	27.9	215	1.599	5.08	3.110(+/-0.019)
FDC	CCD12	0.95	Quartz very fine sand	13	29.5	199	1.455	3.269	2.180(+/-0.012)
FDC	CCD13	1.2	Quartz fine sand	10.5	22.88	96.8	1.007	2.86	2.770(+/-0.014)
FDC	CCD14	1.3	Quartz fine sand	45.2	32.8	471	2.75	62.3	22.600(+/-0.012)
FDC	CCD17	0.7	Quartz fine sand	38	26.5	372	2.283	12.44	5.380(+/-0.032)
FDC	CCD19	0.7	Quartz fine sand	10.9	11.3	321	1.47	34.3	23.300(+/-0.018)
FDC	CCD20	0.7	Quartz fine sand	11	13.9	93.9	0.878	11.29	12.790(+/-0.074)
FDC	CCD21	0.75	Quartz fine sand	8.22	7.09	165	0.919	13.84	14.990(+/-0.091)
SGB	CCD1	1.8	Quartz fine sand	43.5	43	532	3.05	8.87	2.840(+/-0.013)
SGB	CCD5	1.1	Quartz fine sand	27.26	22.57	239	1.661	21.23	12.710(+/-0.073)
SGB	CCD8	1.1	Quartz fine sand	26.8	23.22	242	1.673	9.91	5.850(+/-0.034)
SGB	CCD11	1.7	Quartz fine sand	29.31	25.12	350	2.025	58.6	28.900(+/-0.014)

7
 8 Where charcoal was present in a substantial number at the base of the depression fill, a sample was
 9 taken and analysed for ¹⁴C dating. Four calibrated age intervals were obtained, with medians of 4306,
 10 2500, 2128 and 1936 yrs BP (Table 2). All datings were within the second half of the Holocene.

1 FDC-CCD3 was dated by both OSL and ^{14}C , yielding 2400 yrs BP and 2500 cal. yrs BP respectively. The
 2 two methods therefore provided very consistent ages for the fill in this depression. The fill in the
 3 FDC-CCD17 depression was also doubly dated. The OSL age obtained was 5380 BP while the ^{14}C age
 4 was 4306 cal. yrs BP. The difference is greater but the two dates are still relatively close if we
 5 consider the distribution of all the dates obtained.

6 **Table 2** Results of ^{14}C dating for charcoal from CCD infillings. The calibrated ^{14}C dates given are
 7 intervals of calendar years, encompassing the true age of the samples with a probability of ca. 95%.
 8 The calibration was done with the OxCal software (OxCal v4.4.2 Bronk Ramsey (2009); r:5 Atmospheric
 9 data from Reimer et al. (2020)).

Forest	CCD n°	Depth(m)	Material	^{14}C Age BP	Calibrated age (OxCal 4.4) Probability intervals	Median age cal. BP
FDC	CCD3	1.4	Charcoal	2440 ±35	594BC (59.6%) 407BC	2500
FDC	CCD11	1.9	Charcoal	1985 ±30	44BC (86.4%) 85AD	1936
FDC	CCD16	0.9	Charcoal	2135 ±30	206BC (81.2%) 51BC	2128
FDC	CCD17	0.9	Charcoal	3845 ±30	2410BC (86.1%) 2203BC	4306

10 Of the 25 CCDs likely to be former limestone quarries, 16 have been dated. Of the 16 CCDs dated, six
 11 (FDC-CCD14, 19, 20, 21; SGB-CCD5, 11) had a fill that predated the early Holocene which excludes them
 12 from being limestone quarries contemporary with agricultural societies.

13 3.4. Pedogenetic development inside and outside the CCDs

14 The most common soil type found inside the 25 CCDs (Table 3) was Calcaric Cambisol (12/25) followed
 15 by a diverse set of Luvisols (11/25). A few of the soils (FDC-CCD14/ CCD19/ CCD20/ CCD21, SGB-CCD1/
 16 CCD5/ CCD11) had no calcareous characteristics. Of the latter, all but one (SGB-CCD1) had pre-
 17 Holocene infills. In the case of SGB-CCD1, the thick surrounding local decarbonated silt soils could
 18 explain the absence of carbonates in the fill. For Luvisols, the base of the BT horizon often coincided
 19 with fill levels that were still rich in limestone fragments.

20 Outside the CCDs, the most common soil type was Luvisol (16/25), followed by Calcaric Cambisol
 21 (9/25). In several cases (FDC-CCD12 & CCD17, SGB-CCD1), the Luvisols encountered outside the CCDs
 22 had sharper and more clayey subsurface soil horizons (Bt).

1 Regardless of depth (5, 25, 50cm) Wilcoxon rank tests returned non-significant differences in pH_{water}
 2 values between inside and outside the CCDs (Table 4).

3

4 **Table 3** Classification (IUSS Working Group WRB, 2015) of soils and underlying rocks, inside and outside
 5 the 25 surveyed CCDs (candidate CCDs for marls pits). Light orange indicates CCDs without the
 6 diagnostic features of a limestone quarry.

7

Forest	N° CCD	Soil (& Horizons) inside CCD	Soil (& Horizons) outside CCD
FDC	1	Rendzic Leptosol (Aca, Rca)	Endoleptic Luvisol (A, E, BT, Mca, Rca)
FDC	2	Luvic Endocalcaric Cambisol (A, BT, Cca, Rca)	Endoleptic Luvisol (A, E, BT, Mca, Rca)
FDC	3	Luvic Calcaric Cambisol (A, S/BT, Cca, Rca)	Endoleptic Luvisol (A, E, BT, Mca, Rca)
FDC	4	Calcaric Cambisol (Aci, Sca, Cca, Rca)	Endoleptic Luvisol (A, S/E, BT, Mca, Rca)
FDC	5	Leptic Calcaric Cambisol (Aci, Sca, Cca, Rca)	Epileptic (truncated) Luvisol (A, BT, Mca, Rca)
FDC	6	Endoleptic Calcaric Cambisol (A, Sci, Sca, Cca, Mma)	Epileptic Calcaric Cambisol (Aci, Sca, Mca, Mma)
FDC	7	Calcaric Cambisol (A, Sca, Mma)	Ferric Cambisol (A, S, S à sequioxydes; buried Calcaric Paleogley A, Bgca, Mca)
FDC	8	Calcaric Cambisol (Aca, Bca, Mca)	Epileptic Calcaric Cambisol (Aci, Sca, Cca, Mca)
FDC	9	Calcaric Cambisol (A, Sca, Rca)	Endoleptic Calcaric Cambisol (Aci, Sca, Cca, Mca)
FDC	10	Endoleptic Calcaric Cambisol (A, Sca, Rca)	Endoleptic Calcaric Cambisol (Epiclayic) (A, Sca, BTca, Rca)
FDC	11	Luvisol (Siltic) (A, E, BT, C) over buried Pretic Anthrosol (Leptic Calcaric) (Aca, Rca)	Epileptic (truncated) Luvisol (A, BT, Mca, Rca)
FDC	12	Endoleptic Endocalcaric Luvisol (A, E, BTca, Rca)	Endoleptic Luvisol (A, E, BT, Mca, Rca)
FDC	13	Calcaric Cambisol (A, S, Sca, Mma)	Luvisol (A, E1, E2, BT, Mca, Mma)
FDC	14	Luvisol (Siltic) (A, E, BT1, BT2, C, R)	Luvisol (Siltic) (A, E, BT1, C, BT2, R)
FDC	16	Calcaric Cambisol (A, Sca, Rca)	Epileptic Calcaric Cambisol (Aca, Sca, Mca, Rca)
FDC	17	Endoleptic Luvisol (A, E, BT, Rca), rounded and isolated limestone blocks inside BT	Luvisol (A, E, BT, Mca, Rca)
FDC	18	Calcaric Cambisol (Aca, Sca, Cca, Rca)	Epileptic Calcaric Cambisol (Aca, Sca, Mca, Rca)
FDC	19	Albic Protospodic Dystric Arenic Luvisol (A, E, BP, BT, Msi)	Albic Dystric Arenic Luvisol (A, E, BT, Mma, Mca, Msi)
FDC	20	Endoleptic Arenic Luvisol (Pretic) (A, E, BT, Mca)	Endoleptic Arenic Luvisol (A, E, BT, Mca)
FDC	21	Arenic Dystric Luvisol (A, E1, E2, BT, Msi/Mca)	Arenic Dystric Luvisol (A, S, BT, Mca, Msi/Mca)
SGB	1	Gleyic Luvisol (Siltic Pretic) (A, Bi, Btg1, Btg2, C, Cca)	Luvisol (Siltic) (A, E, BT, C, Cca)
SGB	4	Epileptic Calcaric Cambisol (Aca, Sca, Rca)	Epileptic Calcaric Cambisol (Aci, Sca, Rca)
SGB	5	Chromic Luvisol (A, E, BT, Cca/C, Rca)	Endoleptique Luvisol (A, E, BT, Mca, Rca)

SGB	8	Luvisol (Arenic) (A, E, BT, Rca) with rounded and isolated limestone blocks inside BT	Epileptic Calcaric Cambisol (Aca, Sca, Mca, Rca)
SGB	11	Luvisol (Siltic) over Gleysol (A, E, BT, C, Cg)	Luvisol (Siltic) over Gleysol (A, E, BT, C, Cg, Cca)

1

2 **Table 4** Comparative results of soil pH_{water} analyses inside and outside the 25 CCDs.

Soils Depths (cm)	pH_{water} inside CCDs	pH_{water} outside CCDs	Wilcox.test
-5	5.70	5.36	0.2348
-25	5.91	5.94	0.5416
-50	6.29	6.40	0.925

3

4 Several CCDs (FDC-CCD11, CCD12, CCD16, SGB-CCD1) also contained pieces of ancient A, S, E and BT
5 horizons mixed with limestone fragments in the lower part of their fill. During the digging of the soil
6 pits, these pieces of ancient horizons were distinguishable by clear boundaries between blocks of
7 different colours and textures. They disappeared progressively in the upper part of the fill, particularly
8 in the 50 cm just below the surface. The frequency of bioturbation in the superficial part of the present-
9 day soils could explain the disappearance of these very friable fragments with fine matrices through
10 homogenisation. After this homogenisation, only the limestone fragments, if they have not been
11 dissolved by the surface acidification of the soil, still bear witness to the diversity of origins of the infill
12 materials.

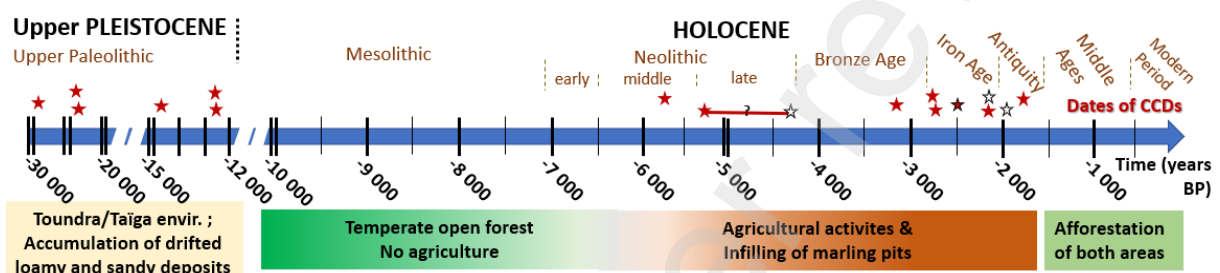
13

14 **4. Discussion**

15 **4.1. A minority of natural depressions with pre-Holocene infill and a majority of limestone quarry** 16 **(potential marl pits)**

17 The fill of six CCDs dated back from Late Glacial Maximum (LGM) to Younger Dryas (Fig. 5) match the
18 age of aeolian sandy (FDC-CCD19, CCD20, CCD21, SGB-CCD5) or silty (FDC-CCD14, SGB-CCD11) deposits
19 and miss artefacts from Holocene agricultural societies as well as scattered carbonate rock fragments.

1 These depressions are likely natural. Several hypotheses can explain how they trapped sediments
 2 during the last Ice Age, but two are more plausible, namely thermokarst depressions in a context of
 3 wind-blown sands and loessic silts (for FDC-CCD14, 19, 20, 21 and SGB-CCD11); and suffosion due to
 4 the strong irregularities in the depth of the limestone/fill interface (for SGB-CCD5, located on a
 5 limestone plateau). Alternative hypotheses include various natural processes leading to CCD formation
 6 in the European loess belt (see for example Kołodyńska-Gawrysiak et al., 2017), like piping erosion,
 7 irregularities in the deposition of aeolian sediments, deflation hollows (Gillijns et al., 2005).



8 Fig. 5. OSL (before 1950) and Carbon-14 (cal. BP) dating results of the CCD infill integrated into a (non-
 9 linear) time scale with the chronocultural periods. OSL dates are indicated by a red star, while ¹⁴C dates
 10 are indicated by a white star with a black border. The two symbols are combined if the two dates are
 11 almost identical for the same CCD.
 12

13 According to the age of infilling, 10/16 of CCDs date back to the second half of the Holocene (Fig. 5)
 14 and correspond to potential marl pits. They span time periods from the Middle Neolithic, to the Bronze
 15 and Iron Ages, to the Roman antiquity. This is consistent with the time at which both forests started to
 16 establish on these former agricultural lands, i.e. the end of antiquity (de Tours, 1836; Fremont and
 17 Woimant, 1976, 1975; Pichon, 2002; Thuilliers, 2017; Tuffreau-Libre, 1977; Acta Sanctorum, Vita Sancti
 18 Gobani). The earliest potential marl pit we found date back to the Middle Neolithic, hence it is 2000
 19 years older than marl pits dated by Rommens et al. (2007) from the Middle Bronze Age.

20 **4.2. Limestone quarry infilling and pedogenesis**

1 The nine potential marl pits showing a single-phase filling suggests intentional filling immediately after
2 reclamation of the quarry, plausibly with the aim of rehabilitating it into agricultural lands. A similar
3 observation was reported by Gillijns et al. (2005) and Poesen et al. (2018), who identified carbonate
4 rock quarries filled that had been more or less levelled depending on their location in the field or under
5 forest cover in central Belgium. However, in their case the filling was not single-phased but composed
6 of several successive layers of colluvium. Our sole exception was site FDC-CCD11 which showed a
7 paleosol at the basis on a thin, likely natural fill. It indicates a delay between the abandonment of the
8 quarry and the infilling operation.

9 In contrast, FDC-CCD1 is an abandoned quarry with no previous infilling; therefore, the thin existing fill
10 is probably natural. This CCD allows to observe the natural functional morphology (bowl shape, steep
11 slopes) and provides a model for the other local CCDs. The same CDD showed an well-preserved edge
12 with a levelled slope and a buried compacted surface which might have been an access ramp to the
13 bottom of the quarry. It is thus likely that this quarry has been abandoned at the same time as
14 agricultural activities, before the land became afforested (4th to 5th century AD).

15 Carbonate rock fragments dispersed in a matrix of earth were retrieved in the lower half of the filling
16 of 0/6 natural CCDs and 9/10 of potential marl pits, consistent with their hypothesized use as quarries.
17 Among The notable exception is site SGB-CCD1 which contained loess with 10-15% calcium carbonate,
18 where soil acidification may have more rapidly eliminated the remnants of this fine and weak
19 carbonate component in the filling. The absence of carbonate rock fragments near the surface can be
20 due to soil acidification (from the surface) after the afforestation of these territories (Brasseur et al.,
21 2018). Applying the criteria of presence of carbonate rock fragments and artefacts of ancient agrarian
22 societies in the fill, there are out of 25 CCDs with a limestone gap (on the inner side), 19 quarries (&
23 marl pit candidates).

24 We conclude that in the northern part of the Paris Basin nearly 75% of the CCDs associated with a
25 carbonate gap are former carbonate rock quarries now filled with a mixture of carbonate materials.

1 Without the help of a DTM Lidar, these advanced Technosols, with frequently Calcaric, Leptic, Cambic
2 or Luvic diagnostic horizons can easily be considered as calcaric cambisols or a rendzic leptosols at first
3 glance. Considering the long history of local agriculture and anthropogenic erosion, the soils
4 surrounding these CCDs can often be classified as Anthrosols.

5 The thicker and more calcareous soils inside former quarries compared to soils outside (Table A.2), as
6 well as the less pronounced horizonation (cf. rarity of clay (BT) and albic (E) horizons) can be explained
7 by the relatively young age of the parent material and thus to less advanced depletion/enrichment
8 processes.

9 In the absence of ancient marling activities and erosion due to agriculture, the soils encountered in the
10 areas studied would have been Albic Stagnic Fragic Luvisols and Dystric Cambisols depending on the
11 depth of the limestone substrate. Such soils are now only found at the bottom of the slope, buried
12 under the thick colluvium of the first phases of cultivation. In areas covered by quartz drifted sands,
13 Albic Podzosols are expected to dominate. Where these sands reach significant thicknesses and in the
14 absence of nearby calcareous substrates the dunes formed have sometimes been spared by agriculture
15 and these soils are then preserved (Horen et al., 2015).

16 **4.3. Materials suitable for marling extracted from quarries and archeogeographic distribution**

17 Where several carbonate rock types were locally accessible, as in our study area, extraction was
18 priority done on the most friable carbonate layers with low clay content. Once those extracted,
19 extraction often stopped on a hard limestone (FDC-CCD1, CCD2, CCD3, CCD4, CCD5, CCD9, CCD10,
20 CCD11, CCD12, CCD16, CCD17; SGB-CCD4, CCD8) or a marl (FDC-CCD7, CCD13). This further supports
21 the hypothesis that these former quarries were used for carbonate amendment in surrounding
22 agricultural lands, though secondary uses cannot be fully ruled out (e.g. paving of roads and paths,
23 mortar). Compared to the situations observed in central Belgium (Poesen et al., 2018), carbonate loess
24 was rarely used in our study area, probably because more suitable and/or more accessible substrates
25 (e.g. CaCO₃-rich limestone rocks below a thin layer of silt) were accessible in our case.

1 We therefore favour the hypothesis that these depressions are indeed old marl pits rather than
2 carbonate quarries of undetermined use. The spatial layout of the most recent marl pits supports this
3 hypothesis since they were clearly integrated into the agrarian plots (see appendix Fig.A4). Another
4 striking feature is the high density of quarries in a limited area. On the Compiègne forest southern
5 plateau, each unit of land (from 5 to 13 ha) had its own marl pit. This illustrates the importance in the
6 past of avoiding the cost of transporting large volumes of the local limestone. Marl pits were therefore
7 much more abundant features in earlier agrarian landscapes.

8 **4.4. How old is the alkaline revolution in the north-western European soilscapes?**

9 Here we provided robust diagnostic criteria to distinguish former carbonate rocks quarries among
10 lidar-detected CDDs: i) the presence of carbonate rocks fragments in the fill matrix; ii) dating to the
11 second half of the Holocene; and iii) the presence of other artefacts associated with agricultural
12 societies.

13 Compared to other continents, Europe has the highest proportion of carbonate-containing rocks near
14 the surface (Hartmann and Moosdorf, 2012). Most of North-West Europe agricultural soils are
15 currently affected by marling or more modern alkaline amendments, which has an enormous
16 influence on their physico-chemical and biological processes (Goulding, 2016; Griffiths et al., 2016;
17 Jauzein, 2011; Turbé et al., 2010; Winiwarter and Blum, 2008). This widespread practice is much
18 more deeply rooted in our agricultural history than previously thought. It has also contributed to
19 structure ancient agrarian landscapes for several thousand years. The legacy on pedological
20 processes and edaphic ecosystems is still very important (Brasseur et al., 2018; Dambrine et al.,
21 2007), even on territories considered to be little impacted, such as circa. 1.6 millenia old forests
22 (Dupouey et al., 2002). More studies are needed to better measure the temporal depth of this
23 anthropic influence in order to better model the long-term influence on the evolutionary trajectories
24 of soils and associated ecosystems (Ewald, 2003). Still our results support the hypothesis of an
25 “alkaline soil revolution” at the Neolithic period, which primarily affected siliceous soils sensitive to

1 natural acidification due to humid climate conditions (Slessarev et al., 2016) when a limestone
2 substrate was present nearby. It is likely that this alkaline revolution deviated these acidic soils
3 durably from their natural evolutionary trajectory.

4

5 **Acknowledgements**

6 The authors would like to thank the French Ministère de la Culture which funded the ARPEGE project.
7 We also thank the Office National des Forêts for its support of the project, in particular for making the
8 Lidar available on the two forests. Thanks to Guillaume Decocq for his careful proofreading and Yves
9 Le Bechennec for his help in the chronocultural determination of pottery fragments.

10 **References**

- 11 Baumewerd-Schmidt, H., Gerlach, R., 2001. Von Restfundstellen und Scheinfundstellen-Ergebnisse
12 einer Grabenbetreuung in der Lösslandschaft., in: Archäologische Informationen. pp. 13–19.
- 13 Brasseur, B., Horen, H., Buridant, J., 2015. Dynamiques d'évolution des luvisols suivant leurs histoires
14 agricole et forestière. *Revue du Nord, Art et Archéologie* 105–112.
- 15 Brasseur, B., Spicher, F., Lenoir, J., Gallet-Moron, E., Buridant, J., Horen, H., 2018. What deep-soil
16 profiles can teach us on deep-time pH dynamics after land use change? *Land Degradation &*
17 *Development* 29, 2951–2961. <https://doi.org/10.1002/ldr.3065>
- 18 Chauchan, R.P., 2014. Role of Earthworms in Soil Fertility and Factors Affecting Their Population
19 Dynamics: A review. *International Journal of Research* 1, 642–649.
- 20 Climate-data.org, n.d. Climate data [WWW Document]. URL <https://fr.climate-data.org/> (accessed
21 2.20.19).
- 22 Clout, H.D., Phillips, A.D.M., 1972. Fertilisants minéraux en France au XIXe siècle. *Études rurales* 45,
23 9–28. <https://doi.org/10.3406/rural.1972.1708>
- 24 Dambrine, E., Dupouey, J.-L., Laüt, L., Humbert, L., Thinon, M., Beauvils, T., Richard, H., 2007. Present
25 Forest Biodiversity Patterns in France Related to Former Roman Agriculture. *Ecology* 88,
26 1430–1439. <https://doi.org/10.1890/05-1314>
- 27 David, S., Dardignac, C., 2018. Rapport de synthèse des prospections archéologiques d'après les
28 données lidar. Forêt domaniale de Compiègne (Oise). Office National des Forêts.
- 29 de Tours, G., 1836. *Historiae ecclesiasticae francorum - Histoire ecclésiastique des Francs*, livre IV,
30 Société d'Histoire de France. ed. Joseph Guadet, Paris.
- 31 Delafosse, W., 1948. De l'origine des mardelles de Lorraine. *Mémoire de l'Académie nationale de*
32 *Metz* 11, 63–85.
- 33 Dupouey, J.L., Dambrine, E., Laffite, J.D., Moares, C., 2002. Irreversible impact of past land use on
34 forest soils and biodiversity. *Ecology* 83, 2978–2984. [https://doi.org/10.1890/0012-](https://doi.org/10.1890/0012-9658(2002)083[2978:IIOPLU]2.0.CO;2)
35 [9658\(2002\)083\[2978:IIOPLU\]2.0.CO;2](https://doi.org/10.1890/0012-9658(2002)083[2978:IIOPLU]2.0.CO;2)
- 36 Etienne, D., Ruffaldi, P., Goepf, S., Ritz, F., Georges-Leroy, M., Pollier, B., Dambrine, E., 2011. The
37 origin of closed depressions in Northeastern France: A new assessment. *Geomorphology* 126,
38 121–131. <https://doi.org/10.1016/j.geomorph.2010.10.036>

- 1 Ewald, J., 2003. The calcareous riddle: Why are there so many calciphilous species in the Central
2 European flora? *Folia Geobot* 38, 357–366. <https://doi.org/10.1007/BF02803244>
- 3 Fremont, J.-M., Woimant, B., 1976. Le vicus gallo-romain de la Carrière du Roi en forêt de Compiègne
4 (Oise), 2e partie. *Revue Archéologique de l'Oise* 45–49.
- 5 Fremont, J.-M., Woimant, B., 1975. Le vicus gallo-romain de la Carrière du Roi en forêt de Compiègne
6 (Oise), 1e partie. *Revue Archéologique de l'Oise* 44–46.
- 7 Galbraith, R.F., Roberts, R.G., Laslett, G.M., Yoshida, H., Olley, J.M., 1999. Optical Dating of Single and
8 Multiple Grains of Quartz from Jinmium Rock Shelter, Northern Australia: Part I,
9 Experimental Design and Statistical Models*. *Archaeometry* 41, 339–364.
10 <https://doi.org/10.1111/j.1475-4754.1999.tb00987.x>
- 11 Gillijns, K., Poesen, J., Deckers, J., 2005. On the characteristics and origin of closed depressions in
12 loess-derived soils in Europe—a case study from central Belgium. *CATENA* 60, 43–58.
13 <https://doi.org/10.1016/j.catena.2004.10.001>
- 14 Goulding, K.W.T., 2016. Soil acidification and the importance of liming agricultural soils with
15 particular reference to the United Kingdom. *Soil Use Manage* 32, 390–399.
16 <https://doi.org/10.1111/sum.12270>
- 17 Griffiths, R.I., Thomson, B.C., Plassart, P., Gweon, H.S., Stone, D., Creamer, R.E., Lemanceau, P.,
18 Bailey, M.J., 2016. Mapping and validating predictions of soil bacterial biodiversity using
19 European and national scale datasets. *Applied Soil Ecology, Soil biodiversity and ecosystem*
20 *functions across Europe: A transect covering variations in bio-geographical zones, land use*
21 *and soil properties* 97, 61–68. <https://doi.org/10.1016/j.apsoil.2015.06.018>
- 22 Guérin, B., Pomerol, C., Salin, R., 1975. Carte Géologique de la France à 1/50 000: Villers-Cotterêts.
- 23 Hartmann, J., Moosdorf, N., 2012. The new global lithological map database GLiM: A representation
24 of rock properties at the Earth surface. *Geochemistry, Geophysics, Geosystems* 13.
25 <https://doi.org/10.1029/2012GC004370>
- 26 Horen, H., Brasseur, B., Feiss, T., Héraude, M., Buridant, J., Gallet-Moron, E., Rassat, S., Montoya, C.,
27 Burban-Col, V., 2015. Relation entre les structures archéologiques identifiées sur un levé
28 LIDAR et la typologie des sols du massif forestier de Compiègne (Nord de la France). *Revue*
29 *du Nord* 85–94.
- 30 IUSS Working Group WRB, 2015. World Reference Base for Soil Resources 2014, update 2015
31 International soil classification system for naming soils and creating legends for soil maps.
32 FAO, Rome.
- 33 Jauzein, P., 2011. Flore des champs cultivés. Editions Quae, Versailles.
- 34 Juo, A.S.R., Manu, A., 1996. Chemical dynamics in slash-and-burn agriculture. *Agriculture, Ecosystems*
35 *& Environment, Alternatives to Slash-and-Burn Agriculture* 58, 49–60.
36 [https://doi.org/10.1016/0167-8809\(95\)00656-7](https://doi.org/10.1016/0167-8809(95)00656-7)
- 37 Kołodyńska-Gawrysiak, R., 2019. Holocene evolution of closed depressions and its relation to
38 landscape dynamics in the loess areas of Poland. *The Holocene* 29, 543–564.
39 <https://doi.org/10.1177/0959683618824792>
- 40 Kołodyńska-Gawrysiak, R., Poesen, J., 2017. Closed depressions in the European loess belt – Natural
41 or anthropogenic origin? *Geomorphology* 288, 111–128.
42 <https://doi.org/10.1016/j.geomorph.2017.02.004>
- 43 Läuchli, A., Grattan, S.R., 2017. Plant stress under non-optimal soil pH, in: *Plant Stress Physiology*,
44 2nd Edition. CABI, pp. 201–2016.
- 45 Lenoir, J., Gril, E., Durrieu, S., Horen, H., Laslier, M., Lembrechts, J.J., Zellweger, F., Alleaume, S.,
46 Brasseur, B., Buridant, J., Dayal, K., De Frenne, P., Gallet-Moron, E., Marrec, R., Meeussen, C.,
47 Rocchini, D., Van Meerbeek, K., Decocq, G., 2022. Unveil the unseen: Using LiDAR to capture
48 time-lag dynamics in the herbaceous layer of European temperate forests. *Journal of Ecology*
49 110, 282–300. <https://doi.org/10.1111/1365-2745.13837>
- 50 Leroyer, C., 2006. L'IMPACT DES GROUPES NÉOLITHIQUES DU BASSIN PARISIEN sur le milieu végétal:
51 évolution et approche territoriale d'après les données polliniques, in: *Impacts Interculturels*

- 1 Au Néolithique Moyen. S.A.E., Actes du 25e Colloque interrégional sur le Néolithique, Dijon,
2 pp. 131–149.
- 3 Leroyer, C., Barracand, G., Coussot, C., Werthe, E., Hulin, G., Jude, F., Leduc, C., Allenet de Ribemont,
4 G., 2017. Nouvelles données sur le paysage végétal de la moyenne vallée de l'Oise au
5 subboréal : l'étude de la séquence organique de Thourotte (Oise, France). *Quaternaire. Revue*
6 *de l'Association française pour l'étude du Quaternaire* 471–489.
7 <https://doi.org/10.4000/quaternaire.8469>
- 8 Matthew, W.M., 1993. Marling in British agriculture: a case of partial identity. *Agricultural History*
9 *Review* 41, 97–110.
- 10 Meylemans, E., Vanmontfort, B., Van Rompaey, A., 2014. The evaluation of archaeological sites using
11 LIDAR and erosion/sedimentation modelling. *The Archaeology of Erosion, the Erosion of*
12 *Archaeology, Proceedings of the Brussels Conference, April 28-30, 2008* 23–36.
- 13 Pichon, B., 2002. Carte archéologique de la Gaule 02 : L'Aisne, Carte Archéologique de la Gaule.
14 Académie des Inscriptions et Belles-Lettres.
- 15 Pissart, A., 1958. Les dépressions fermées de la région parisienne. Le problème de leur origine. *Revue*
16 *de Géomorphologie Dynamique* 9, 73–83.
- 17 Poesen, J., Vanwalleghem, T., Deckers, J., 2018. Gullies and Closed Depressions in the Loess Belt:
18 Scars of Human–Environment Interactions, in: *Landscapes and Landforms of Belgium and*
19 *Luxembourg*. Springer, pp. 353–367.
- 20 Prince, H., 1961. Some reflections on the origin of hollows in Norfolk compared with those in the
21 Paris region. *Revue de Géomorphologie Dynamique* 12, 110–117.
- 22 Quénard, L., Samouëlian, A., Laroche, B., Cornu, S., 2011. Lessivage as a major process of soil
23 formation: A revisitation of existing data. *Geoderma* 167–168, 135–147.
24 <https://doi.org/10.1016/j.geoderma.2011.07.031>
- 25 R Development Core Team, 2016. R: A language and environment for statistical computing.
- 26 Ramsey, C.B., 2009. Bayesian Analysis of Radiocarbon Dates. *Radiocarbon* 51, 337–360.
27 <https://doi.org/10.1017/S0033822200033865>
- 28 Reimer, P.J., Austin, W.E.N., Bard, E., Bayliss, A., Blackwell, P.G., Ramsey, C.B., Butzin, M., Cheng, H.,
29 Edwards, R.L., Friedrich, M., Grootes, P.M., Guilderson, T.P., Hajdas, I., Heaton, T.J., Hogg,
30 A.G., Hughen, K.A., Kromer, B., Manning, S.W., Muscheler, R., Palmer, J.G., Pearson, C., Plicht,
31 J. van der, Reimer, R.W., Richards, D.A., Scott, E.M., Southon, J.R., Turney, C.S.M., Wacker, L.,
32 Adolphi, F., Büntgen, U., Capano, M., Fahrni, S.M., Fogtmann-Schulz, A., Friedrich, R., Köhler,
33 P., Kudsk, S., Miyake, F., Olsen, J., Reinig, F., Sakamoto, M., Sookdeo, A., Talamo, S., 2020.
34 The IntCal20 Northern Hemisphere Radiocarbon Age Calibration Curve (0–55 cal kBP).
35 *Radiocarbon* 62, 725–757. <https://doi.org/10.1017/RDC.2020.41>
- 36 Rodet, J., 2010. Les karsts de la craie et du Cénozoïque du bassin de Paris, in: *Grottes et Karsts de*
37 *France, Karstologia-Mémoires*. Association Française de Karstologie, pp. 148–153.
- 38 Rommens, T., Verstraeten, G., Peeters, I., Poesen, J., Govers, G., Van Rompaey, A., Mauz, B.,
39 Packman, S., Lang, A., 2007. Reconstruction of late-Holocene slope and dry valley sediment
40 dynamics in a Belgian loess environment. *The Holocene* 17, 777–788.
41 <https://doi.org/10.1177/0959683607080519>
- 42 Slessarev, E.W., Lin, Y., Bingham, N.L., Johnson, J.E., Dai, Y., Schimel, J.P., Chadwick, O.A., 2016.
43 Water balance creates a threshold in soil pH at the global scale. *Nature* 540, 567–569.
44 <https://doi.org/10.1038/nature20139>
- 45 Slotboom, R.T., van Mourik, J.M., 2015. Pollen records of mardel deposits: The effects of climatic
46 oscillations and land management on soil erosion in Gutland, Luxembourg. *CATENA* 132, 72–
47 88. <https://doi.org/10.1016/j.catena.2014.12.035>
- 48 Thuilliers, P., 2017. Dynamique des paysages de l'Antiquité au Moyen Age. La naissance de la forêt de
49 Compiègne (Ier s. av. J.-C. - XIIIe s. ap. J.-C.). (PhD Thesis). Université de Picardie Jules Verne,
50 Amiens.
- 51 Tuffreau-Libre, M., 1977. La céramique commune gallo-romaine de la forêt de Compiègne (Oise) au
52 Musée des Antiquités nationales. *Cahiers Archéologiques de Picardie* 125–160.

- 1 Turbé, A., Toni, A. de, Benito, P., Lavelle, Patrick, Lavelle, Perrine, Camacho, N.R., Putten, W.H. van
2 D., Labouze, E., Mudgal, S., 2010. Soil biodiversity: functions, threats and tools for policy
3 makers.
- 4 van Mourik, J.M., Braekmans, D.J.G., Doorenbosch, M., Kuijper, W.J., van der Plicht, J., 2016. Natural
5 versus anthropogenic genesis of mardels (closed depressions) on the Gutland plateau
6 (Luxembourg); archaeometrical and palynological evidence of Roman clay excavation from
7 mardels. *SOIL Discussions* 1–44. <https://doi.org/10.5194/soil-2015-82>
- 8 Vanwalleghem, T., Poesen, J., Vitse, I., Bork, H.R., Dotterweich, M., Schmidtchen, G., Deckers, J.,
9 Lang, A., Mauz, B., 2007. Origin and evolution of closed depressions in central Belgium,
10 European loess belt. *Earth Surface Processes and Landforms* 32, 574–586.
11 <https://doi.org/10.1002/esp.1416>
- 12 Winiwarter, V., Blum, W.E.H., 2008. From marl to rock powder: On the history of soil fertility
13 management by rock materials. *Journal of Plant Nutrition and Soil Science* 171, 316–324.
14 <https://doi.org/10.1002/jpln.200625070>
- 15 Young, A., 1808. *Essai sur la nature des engrais*, French translated version. ed. Bertrand, Paris.
16